XI International Conference on Computational Methods in Marine Engineering

MARINE 2025 - Hydrodynamic analysis of a 2MW offshore floating solar farm with breakwater protection

T.H.J. Bunnik[1,*], J. van der Zanden[1] and N. Baderiya[1]

[1] Maritime Research Institute Netherlands,
Haagsteeg 2, 6708PM Wageningen, The Netherlands.

[*] t.bunnik@marin.nl

ABSTRACT

Within the EU project SUREWAVE a new concept for the upscaling of Floating PhotoVoltaics (FPV) to offshore environments is developed. The new concept integrates an existing FPV design with a floating breakwater ring that provides shelter against waves. The system is designed for harsh offshore conditions at sites in the Baltic, Mediterranean and North Seas. A series of model tests was performed with a simplified setup of a 3x5 array of FPV panels behind a floating breakwater. These model tests showed deficiencies in the design of the hinge connections between panels (sensitive to buckling) and lead to an improved hinge design.

The model tests have been used to validate the numerical model of the system based on linear diffraction analysis. The validated numerical model has been used to scale up to a 2MW system (3660 solar panel panels and 32 floating breakwaters) and investigate the effectiveness of the breakwater ring in reducing motions of the panels, loads in the panel connectors (hinges) and wave drift loads on the system. Due to the size of the structure and the large number of floating objects and degrees of freedom the computations have been carried out on a high-performance computer in parallel.

The simulations show that the floating breakwater is capable of reducing the short-wave energy inside the breakwater ring and the related hinge loads, but it may also lead to the development of standing waves inside the breakwater ring. Longer waves are not affected but due to the flexibility of the FPV system the modules follow the wave motions which does not result in high loads. The presence of the floating breakwater leads to a significant increase in wave drift loads. As a consequence, a stronger mooring system needs to be used which is capable of handling these loads.

Keywords: Floating solar; floating breakwater; hydrodynamic analysis; linear diffraction; hinges; model tests; HPC.

1 INTRODUCTION

Offshore Floating PhotoVoltaics (FPV) is gaining increasing attention due to the growth in energy demand, the phasing-out of fossil fuels because of climate change effects and the need for a diverse energy mix to ensure a stable energy supply. Liu Gang et al. (2024) provide an extensive overview of recent offshore FPV developments.

The present study is part of the Horizon Europe project SUREWAVE that aims to upscale FPV concepts to offshore environments. An existing FPV system is adopted (courtesy of Sunlit Sea, Norway). The design, which has passed demonstrations in inland lakes and fjords, consists of 1.88 m x 1.88 m aluminum modules with 0.5 kWp capacity that are interconnected through polyurethane hinges. For upscaling to offshore environments, the FPV system is integrated with an external floating breakwater (FBW) that reduces direct wave loads on the FPV modules.

FBWs are floating structures that attenuate the transmitted wave energy through wave reflection and dissipation due to wave overtopping and viscous losses. The present study considers a common pontoon-type FBW built of concrete. The outcome of the SUREWAVE project is a design of the 2MW FPV farm consisting of 3660 connected FPV panels covering an area of 12936 m^2 and protected by a ring of 32 FBWs, see Figure 1 and Figure *2*.

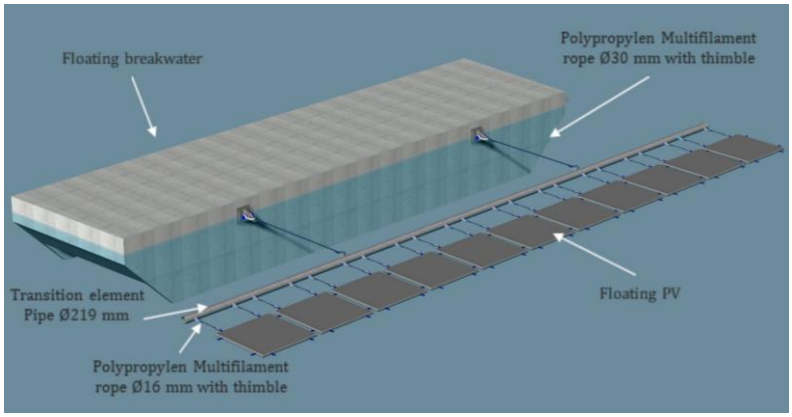

Figure 1: Connection between FBW and FPV with surface mooring ring (courtesy of CLEMENT Germany GmbH).

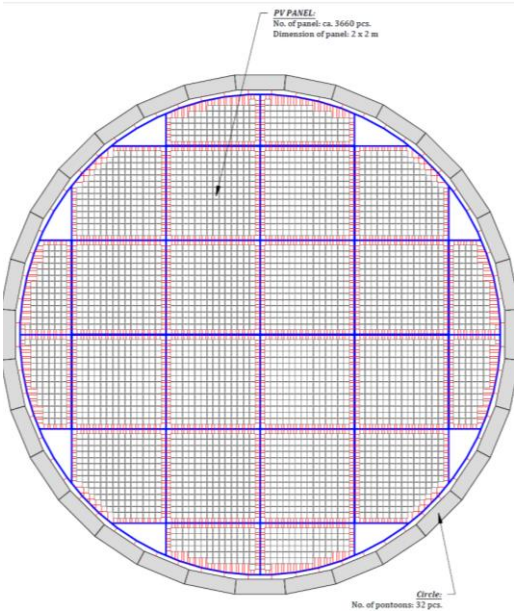

Figure 2: Design of the 2MW farm with FPV arrays, FBW ring and surface mooring (courtesy of CLEMENT Germany GmbH).

The sheer size of the 2MW FPV farm, the complex mechanical couplings between individual floats and the large number of floats/degrees of freedom in the system make it practically infeasible to perform scale model tests for the entire farm. Design performance has to be evaluated using a combination of a) basin tests on a down-sized simplified version of the system; b) numerical model validation using the basin tests; c) numerical simulations on the complete system using the validated model. This approach is also adopted in this paper.

Numerical studies on FPV have been presented by several researchers. A distinction is made between truly flexible systems (i.e. membrane type) and structures consisting of connected rigid floats, like the present SUREWAVE system. Some recent examples from literature are described here. Zhi Yung Tay (2023) presents simulations on a FPV farm protected by a FBW. The multi-modular FPV unit is represented using thin plate theory instead of modeling all individual units. Motions of the plate are represented with mode shapes. Zheng et al. (2020) present simulations for a combined wind–solar–aquaculture system, employing linear diffraction analysis and time-domain simulations. Zhang et el. (2024) present frequency-domain results of a membrane-type floating solar system. They observe that in shortening waves the floater stiffness gains significance, leading to a notable three-dimensional interaction and concerns on the platform's operational performance. Otto et al. (2025) investigate the effects of pontoon dimensions, array size, and hinge stiffness, through a combination of analytical formulations and wave diffraction calculations, validated with basin tests.

Most previous numerical studies focused on relatively small farms (up to tens of pontoons). The present study aims to extend insights into the hydrodynamic performance of a much larger (2MW) offshore FPV farm. The paper presents model tests for a small FPV array (chapter 2), a comparison of those tests with numerical simulations (chapter 3) and finally simulations and observations for the 2MW farm (chapter 4).

2 VALIDATION MODEL TESTS

2.1 Model test setup

Scale model tests in waves were performed for a simplified, down-sized version of the FPV farm, comprising a 3x5 array of FPV panels with a FBW that covers the width of the flume. A first test series was carried out

with hinges between the FPV panels that lacked sufficient compressive stiffness which resulted in buckling (van der Zanden et al, 2024). A second test series was carried out with an improved hinge design that included compressive stiffness. The results of this model test series (measured motions of FPV panels and breakwater) have been used for numerical model validation before scaling up the simulation model to the 2MW farm. Figure 3 shows the basin setup and the hinges between the FPV panels at model scale. For more details on models and basin setup, environmental conditions, and data analysis, see van der Zanden et al. (2024).

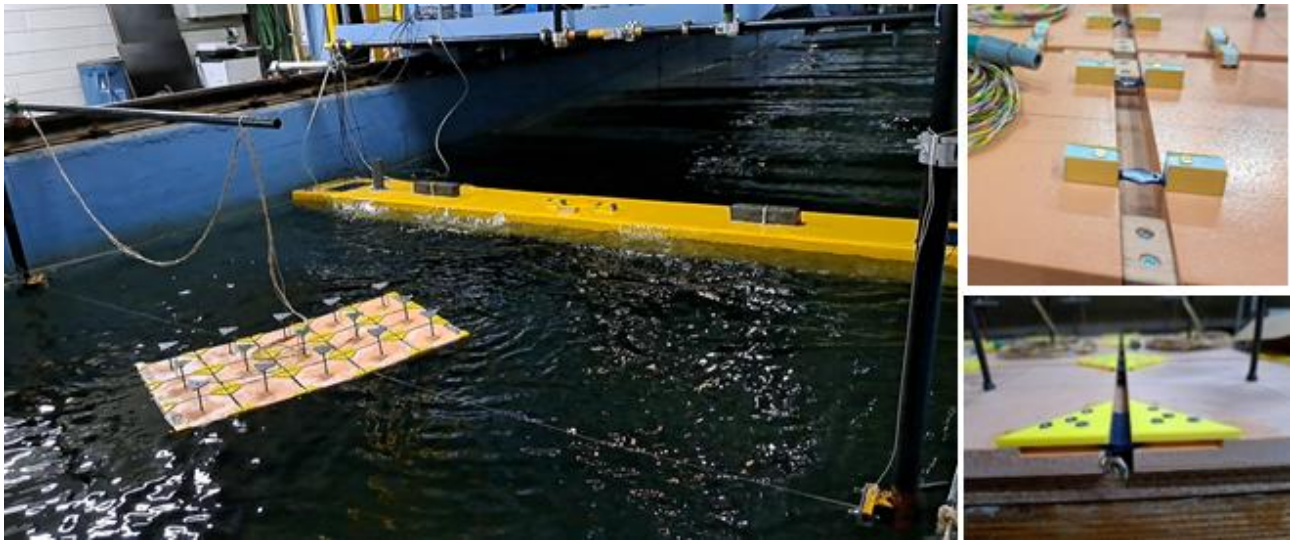

Figure 3: Basin model tests (left), initial hinge design lacking compressive stiffness (top right) and improved hinge design (bottom right).

3 NUMERICAL MODEL VALIDATION

3.1 Linear diffraction theory

Linear multi-body diffraction theory is used to simulate the response of the FPV system to waves. This implies that fluid motions are based on potential flow, so viscous effects and vorticity are neglected. Viscous effects can be added through for example damping in the equations of motions (e.g. roll) or wave dissipation (Bunnik, 2009). An additional assumption is that motions of waves and floating structures are small so boundary conditions on the floats and on the free surface can be linearized. A Boundary Element Method (BEM) is used to solve the Laplace equation and boundary conditions on free surface and surfaces of submerged bodies.

A more detailed description of linear diffraction theory is given in Appendix B.

3.2 Model test comparison

A comparison with the model tests has been made by comparing the Response Amplitude Operator (RAO: the response to a wave of unit amplitude) of the calculated and measured breakwater motions and FPV panels as described in section 2.1.

The main particulars of a FPV panel and the FBW are as follows:

Table 1: Main particulars of a FPV module, including 0.06 m marine growth

Length [m]	1.88		Mass [kg]	346
Width [m]	1.88		Vertical position of Center of Mass [m]	0.10
Height [m]	0.14		Roll/Pitch radius of gyration [m]	0.48
Draft [m]	0.10		Yaw radius of gyration [m]	0.62

Table 2: Main particulars of the FBW

Length [m]	38.0		Mass [tons]	246
Width [m]	5.0		Vertical position of Center of Mass [m]	1.58
Height [m]	2.5		Roll radius of gyration [m]	1.83
Draft [m]	2.03			

The heave and roll damping values of the FBW were derived from the basin decay tests and amount to 8.9% of critical damping for heave and 3.4% of critical damping for roll.

The comparison with the model tests RAOs can be found in Appendix A, both for tests with and without breakwater protection. The following observations can be made:

- The difference in motion response between FPV panels is small.
- The motions of the FPV panels are reduced considerably in short waves due to the presence of the FBW.
- There is a slight mismatch in the RAOs of the floater around the natural period of the breakwater, which is most likely caused by green water overtopping the structure.
- In general there is a good agreement between measurements and calculations. This reaffirms Otto et al. (2025), who validate the same diffraction solver for another design of interconnected floats.

4 SIMULATIONS FOR A 2MW FARM

A 2MW farm was designed by the SUREWAVE consortium. The 2MW farm consists of arrays of solar panels protected by a ring of 32 FBW. The base size of the arrays is 14x14 panels but smaller arrays are used on the outside edge to fit them into the breakwater ring, see Figure 2. FPV panels inside an array are connected by means of the hinges described in chapter 2.1. Arrays are connected to other arrays by means of a surface mooring system. The arrays on the outside edge are connected to a mooring ring which is in turn connected to the breakwater ring. In total, the 2MW farm consists of 3660 FPV panels.

The validated model described in chapter 3.2 is extended and applied to the 2MW farm. Simulations are performed with and without the breakwater ring to quantify the effect of the breakwater ring on the wave transmission and the resulting hinge loads and wave drift loads. The challenge in these simulations is the large number of mesh elements and the large number of degrees of freedom:

- On each FPV panel 45 surface mesh elements are used. Each FBW is modelled with 1500 surface mesh elements. This leads to a total number of 212,700 mesh elements.
- Each FPV panel and each FBW is allowed to move in 6 Degrees of Freedom (DoF), resulting in a total of 22,152 DoFs. For each DoF a radiation potential has to be calculated, resulting in an additional right-hand-side vector in the (linear) system of equations. The radiation potential results in added mass and damping coefficients, including interaction terms between floats.

Because of the large number of DoFs and right-hand-sides in the linear system of equations, the most efficient solver is a direct solver (LU-decomposition). The LU-decomposition has to be made once (for each wave frequency) and the calculation of the solution vector (source strength) for each right-hand-side is relatively cheap. After calculation of the source strength vectors, velocities and pressures on all surface mesh elements are calculated in a post-processing step. Pressures and velocities are subsequently used to calculated added mass, damping and wave force coefficients (first, and second-order wave drift loads). The limiting factor is that the direct solver requires the matrix to be kept in shared memory, so the size of the problem is restricted by the memory of a single compute node of the High Performance Computer used for the simulations. Different wave frequencies can be run in parallel on multiple compute nodes.

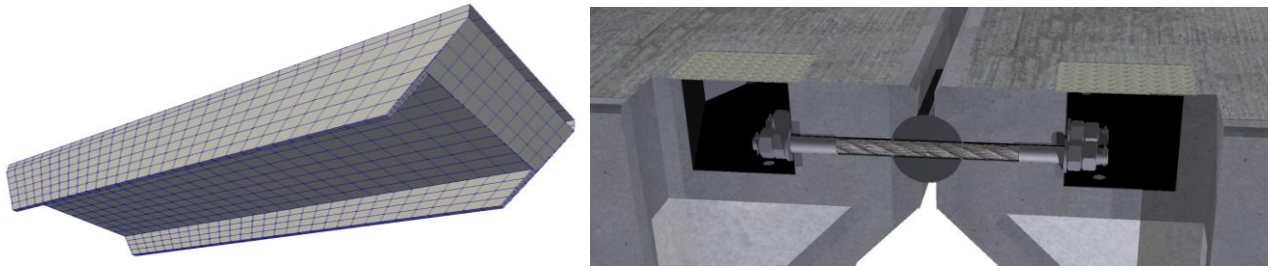

Figure 4: Surface mesh on single FBW (left) and illustration of FBW connection (right). (courtesy of CLEMENT Germany GmbH).

The FBWs are inter-connected with ropes and polymer fenders as illustrated in Figure 4. This leaves the FBWs free to pitch relatively to each other, but other motions are restricted by the stiffness of the connections. In the numerical model this has been modelled as a single spring joint in between the FBWs with a high stiffness in all degrees of freedom, limiting relative motions, except for relative pitch which is left free.

The connection between the FBW and the FPV panels is made by means of a surface mooring ring to which both the FPV panels and the FBW connect with ropes, see Figure 1. The surface mooring should ensure that collisions between FPV panels and the FBW are avoided. The use of either soft or stiff ropes in the surface mooring was investigated, see the discussion on hinge loads (Figure 8).

The combined boundary element mesh of all the FPV panels and the FBWs is shown in Figure 5. Using this mesh the diffraction analysis is run for a wave frequency range from 0.1 rad/s to 3.0 rad/s, with a step of 0.1 rad/s, and for multiple wave directions with a wave direction step of 15 degrees. The calculation time for a single frequency is approximately 16 hours on 24 cores of a HPC, where the majority of the time is spent on:

1. Calculating (Green function) influence coefficients between mesh elements.
2. LU-decomposition of the matrix with influence coefficients and solving for the radiation and diffraction source strengths.
3. Calculation of water pressures and velocities on mesh elements from source strengths and influence coefficients between mesh elements.

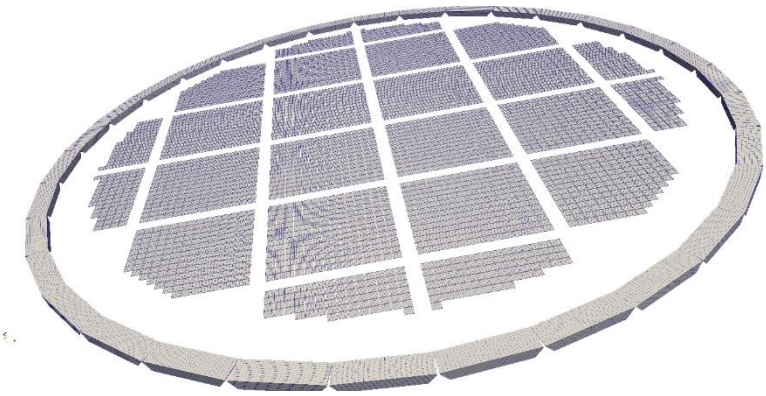

Figure 5: Boundary element mesh on FPV panels and FBWs (212,700 elements in total).

From the pressures and water velocities, the motions of the FPV panels and FBWs, the loads in the hinges and surface mooring, and the wave drift loads have been computed. The downside of using a closed breakwater protection system is that standing waves inside the breakwater ring may start to develop at certain frequencies as is also observed for example in floating fish farms (Verma, 2020). These standing waves are exaggerated in linear diffraction theory and additional free-surface wave damping has to be applied to obtain realistic wave amplitudes as is also commonly done for example in vessel side-by-side simulations, (Chen, 2005), (Bunnik, 2009). Therefore, a free surface damping area was modelled between the breakwater ring and the FPV system, and between the FPV arrays using a non-dimensional damping value of ϵ=0.025 (for its definition see Chen,

2005). Still, at specific frequencies, standing waves inside the breakwater ring were observed, potentially resulting in a local increase of FPV motions and connector loads.

Figure 6 (top panels) shows for example the vertical motion RAO of the farm at a wave frequency of 1.5 rad/s (wave length 27.4 m) with and without the presence of the breakwater ring. Due to standing waves FPV panel motions reduce in nodes but may increase in anti-nodes. Without breakwater ring the panels move more or less up and down with the waves at this wave frequency (RAO is close to 1). For a shorter wave however (wave frequency 2.0 rad/s, see bottom plots in Figure 6) the FBWs are quite effective in reducing FPV panel motions. Also, it can be seen that in the situation without FBW, the FPV panels are not strictly following the waves anymore.

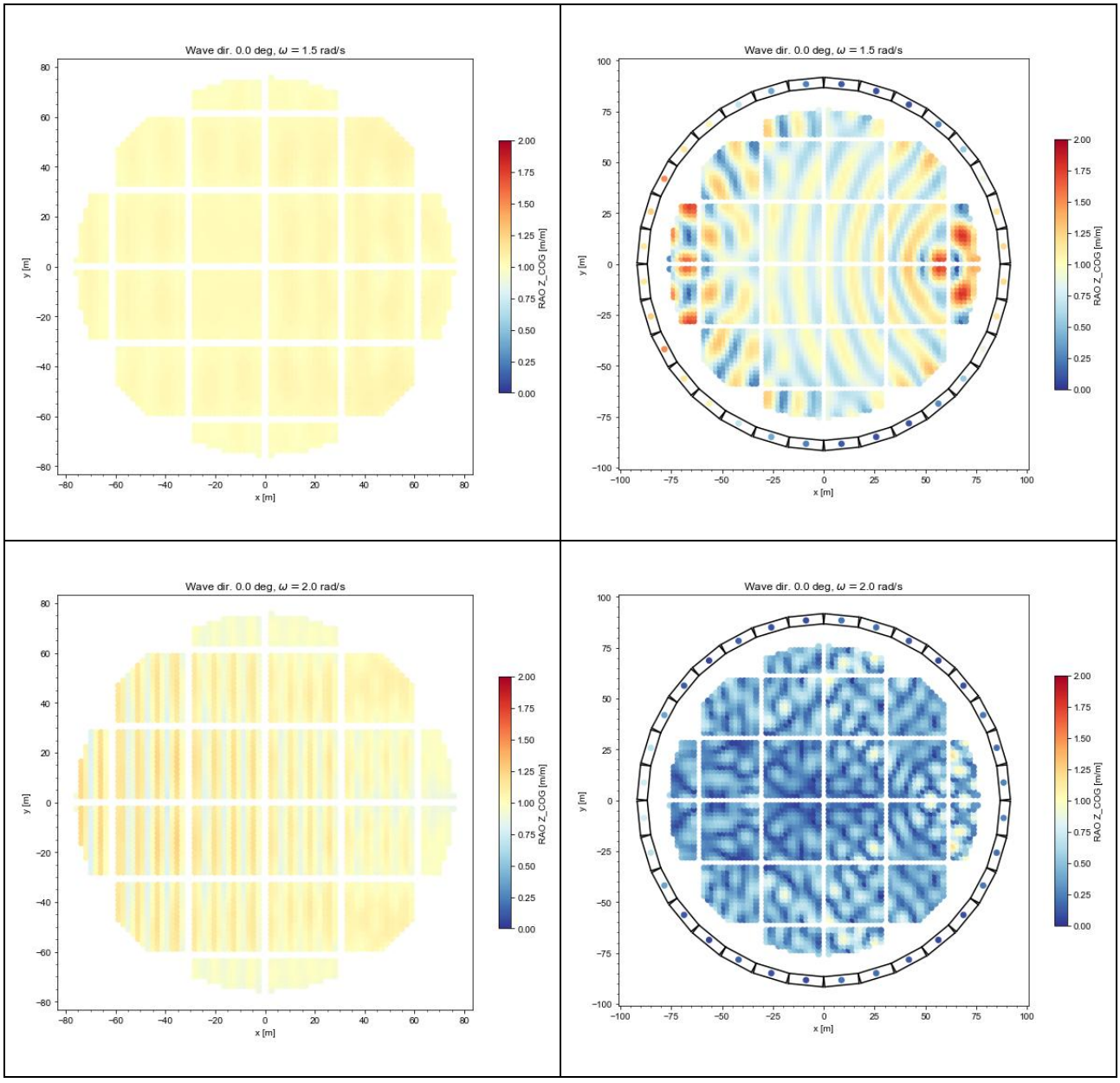

Figure 6: RAOs of vertical motions of bodies at wave frequency 1.5 rad/s (top) and 2.0 rad/s (bottom) without breakwater (left) and with breakwater (right).

The motion responses of the FPV panels were used to calculate relative motions. By multiplying with the hinge stiffness the hinge loads are obtained. Figure 7 shows the normalised RAO of the horizontal hinge load Fx at a wave frequency of 2.0 rad/s. It can be seen that the breakwater helps to reduce the hinge loads for these short waves although some stress concentrations remain especially near the edges of the FPV arrays.

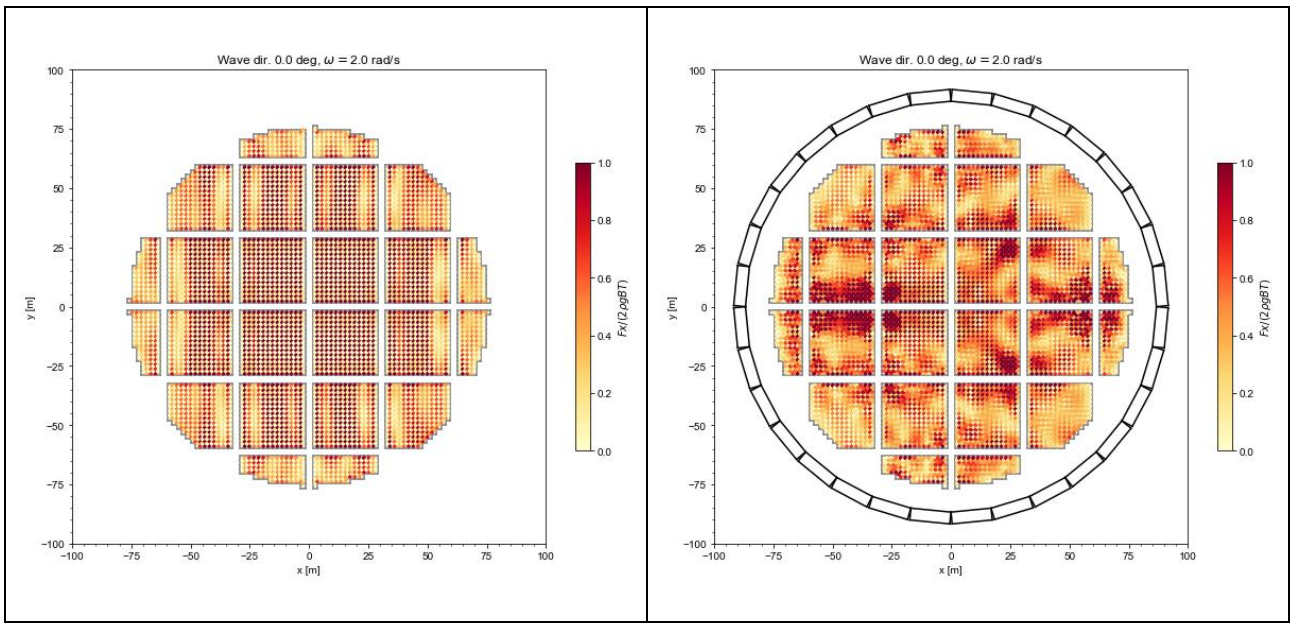

Figure 7: RAOs of normalised horizontal hinge loads Fx at wave frequency 2.0 rad/s without FBW (left) and with FBW (right).

The hinges are susceptible to fatigue loading and exceedance of ultimate strength. Therefore, the RAOs of the hinge loads between FPV panels were used to determine the Most Probable Maximum (MPM) value in North Sea wave conditions following the 50-y return period contour of the intended installation site. The MPM of a linear parameter in a 3-h sea state was calculated based on the linear response amplitude operator (RAO) and the input wave spectrum (S_w) as follows:

$$m_0 = \int S_w(\omega) * RAO(\omega)^2 * d\omega \; ; \; RMS = \sqrt{m_0} \; ; \; MPM = \sqrt{2.\ln N}\,.RMS$$

Where $S_w(\omega)$ is the wave spectrum, m_0 is the zero-order spectral moment of the response spectrum and N represents the number of wave cycles in a 3-hour sea state ($N = 10{,}800/T_z$), where T_z is the zero up-crossing period.

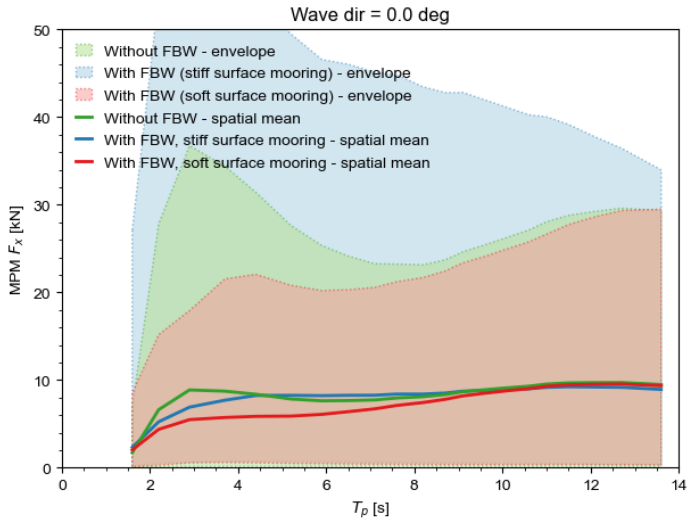

A comparison is made between the situation without FBW, with FBW with a stiff connection between breakwater and the FPV, and with FBW but with a soft connection between breakwater and FPV. The spatial mean of all hinges in the FPV field was calculated as well as the envelope (the maximum value over all hinges), see Figure 8. It can be seen that the stiff breakwater connection leads to higher hinge loads, likely because the loads on the breakwater ring are transferred in to the FPV field and because the horizontal tensioning results in different horizontal modes of the FPV.

Figure 8:Most Probable Maximum (MPM) value hinge loads with and without FBW, with stiff and soft connection between FPV and FBW, for North Sea location.

Using a soft connection the loads are reduced. However, it needs to be investigated if the gap between the breakwater ring and the FPV field is always maintained and collisions are avoided in that case.

The presented hinge MPM load values correspond to the total connection load between 2 adjacent FPV panels. These values can be used to determine the required number of hinges between adjacent panels to ensure that the ultimate loads do not exceed the ultimate strength of a hinge. It should be noted that the results may be sensitive to the applied free-surface damping value. This could be checked with a sensitivity analysis and if needed a more robust estimate of the damping value could be obtained using model tests and/or CFD simulations.

Figure 9 shows the mean wave drift force Quadratic Transfer Function (QTF) on the FPV panels only and on the entire farm (including FBW) with and without the presence of the FBW. Since the FPV is able to follow the waves up to quite high frequencies, the drift forces on the FPV are small, unlike the drift forces on the breakwater ring. It can be seen that the presence of the FBW results in a large increase in drift force, although the wave drift force on the FPV panels decreases. That means that a much heavier and extensive mooring system is needed to keep the farm in place when the breakwater ring is included, resulting in a possible large cost increase.

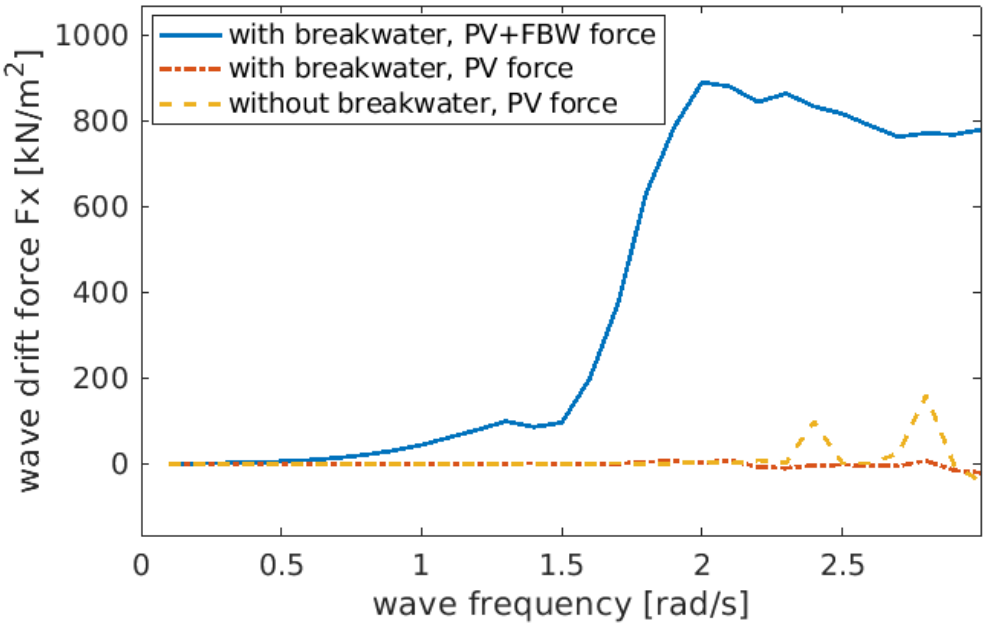

Figure 9: Mean wave drift force on entire 2MW farm with and without FBW presence.

5 CONCLUSIONS

In the EU-funded SUREWAVE project, a 2MW floating solar system protected by a floating breakwater ring was designed. The performance of the system in waves was successfully demonstrated using a combination of model tests and numerical simulations. The model tests were used to validate a numerical model of a simplified and smaller FPV farm. The numerical model was then scaled up to the 2MW farm and the effect of the floating breakwater ring on the connector loads and mooring (wave-drift) forces was investigated. The following conclusions can be made:

- The floating breakwater ring is effective in reducing the expected maximum loads in the hinges between the FPV panels in 50-year North Sea wave conditions, provided that a soft connection is used between the breakwater ring and the FPV panels.
- At specific wave frequencies, standing resonant waves (seiches) may develop in the ring resulting in larger wave-induced motions.

- These standing waves are limited by damping and nonlinear effects (wave breaking, wave overtopping). In the numerical model, this was modelled with a linear free-surface damping value. The results may be sensitive to the applied damping and a sensitivity analysis should be performed. If needed a more robust estimate of the damping value could be obtained using model tests and/or CFD simulations.
- The drift forces on the breakwater ring are much larger than the drift forces on the FPV panels. Introducing the breakwater ring therefore means that a heavier and more expensive seabed mooring is required.

ACKNOWLEDGEMENTS

The present study is part of the SUREWAVE project, Funded by the European Union with GA No. 101083342. Views and opinions expressed are however those of the author(s) only and do not necessarily reflect those of the European Union. Neither the European Union nor the granting authority can be held responsible for them.

REFERENCES

Bunnik, T., Pauw, W., Voogt, A. (2009). Hydrodynamic Analysis For Side-by-Side Offloading. Proceedings of the International Offshore and Polar Engineering Conference.

Chen, X.B. (2005), Hydrodynamic analysis for offshore LNG terminals, Proceedings of the 2nd offshore hydrodynamics symposium, Rio de Janeiro.

Liu, Gang & Guo, Jiamin & Peng, Huanghua & Ping, Huan & Ma, Qiang. (2024). Review of Recent Offshore Floating Photovoltaic Systems. Journal of Marine Science and Engineering. 12. 1942. http://dx.doi.org/10.3390/jmse12111942.

Newman, J.N. (1985). Algorithms for the free-surface green function. J. Eng. Math. 19 (1), 57–67, http://dx.doi.org/10.1007/BF00055041

Otto, W., Kluwer, T. & Hirdaris, S. (2025). Wave induced response of shallow draft interconnected pontoons. Proc. 44th International Conference on Ocean, Offshore and Arctic Engineering, OMAE2025-156362.

Pinkster, J.A. (1979) Low Frequency Second Order Wave Exciting Forces on Floating Structures. PhD thesis, Delft University of Technology.

Verma, A. (2020). Analysis of Sloshing Modes in Floating Fish Farms. Master thesis, NTN.

van der Zanden, J., Bunnik, T., Cortés, A., Delhaye, V., Kegelart, G., Pehlke, T. & Panjwani, B. (2024). Wave Basin Tests of a Multi-Body Floating PV System Sheltered by a Floating Breakwater. Energies. 2024; 17(9):2059. https://doi.org/10.3390/en17092059

Zhang, Yifan & Zhang, Xiantao & Chen, Yongqiang & Tian, Xinliang & Li, Xin. (2024). A frequency-domain hydroelastic analysis of a membrane-based offshore floating photovoltaic platform in regular waves. Journal of Fluids and Structures. 127. http://dx.doi.org/10.1016/j.jfluidstructs.2024.104125

Zheng, Xiangyuan & Zheng, Huadong & Lei, Yu & Li, Junrong & Li, Wei. (2020). An Offshore Floating Wind–Solar–Aquaculture System: Concept Design and Extreme Response in Survival Conditions. Energies. 13. 604. http://dx.doi.org/10.3390/en13030604

Zhi Yung Tay (2023), Performance of Integrated FB and WEC for Offshore Floating Sola Photovoltaic Farm Considering the Effect of Hydroelasticity. J. Mar. Sci. Eng. 2023, 11

APPENDIX A

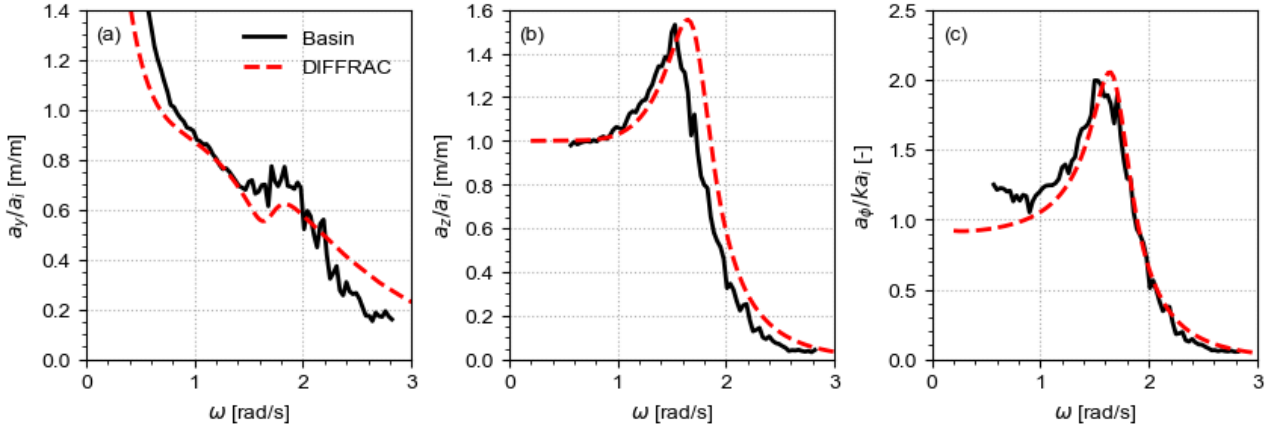

Figure 10: Motion RAOs of floating breakwater: (a) surge; (b) heave; (c) roll. Basin test (solid black) and DIFFRAC (dashed red) results.

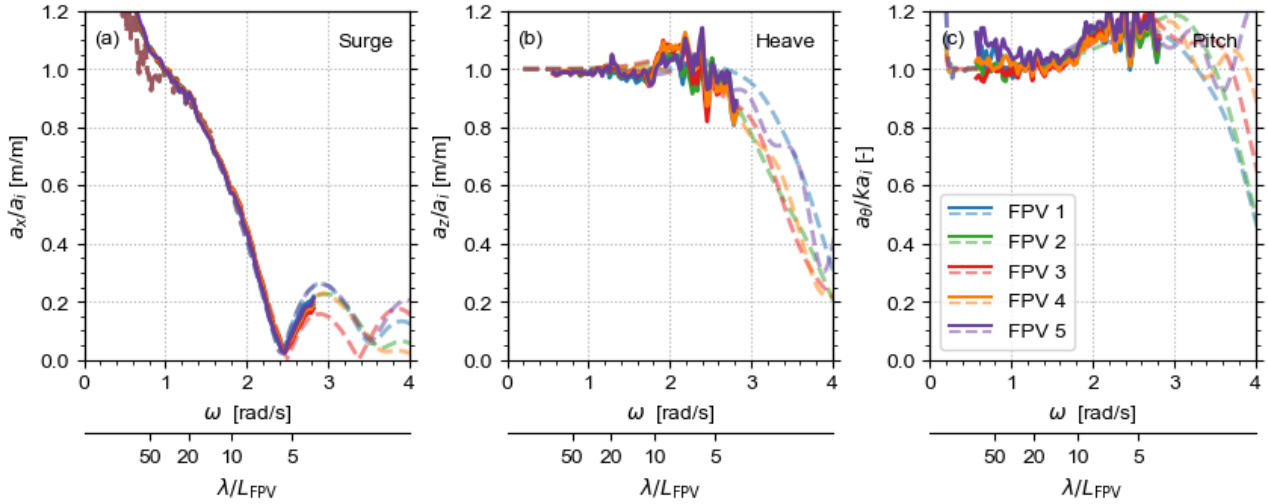

Figure 11: Surge, heave and pitch RAOs in head seas (180 deg) without FBW: DIFFRAC (dashed) and basin results (solid), with different colours marking the five instrumented FPV panels (FPV 1 to FPV 5 is fore to aft).

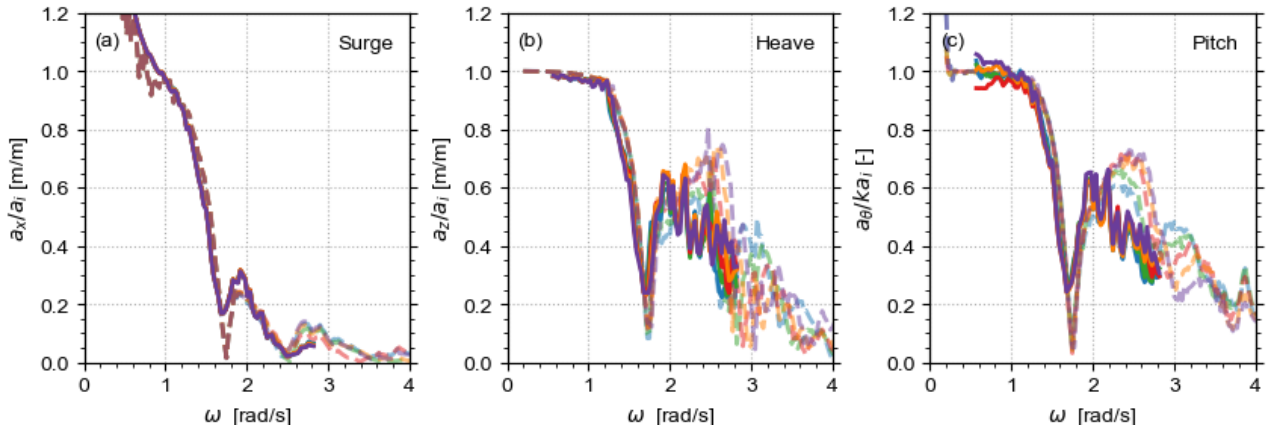

Figure 12: Surge, heave and pitch RAOs in head seas (180 deg) with FBW: DIFFRAC (dashed) and basin results (solid), with different colours marking the five instrumented FPV panels (FPV 1 to FPV 5 is fore to aft).

APPENDIX B

Linear multi-body diffraction theory is used to simulate the response of the FPV system to waves. Because of the linearity assumption, the velocity potential can be split up into individual potentials describing incident waves, radiated waves (added mass, damping effects) and diffracted waves. The potential is then a superposition of these individual potentials:

$$\varphi = \varphi_{inc} + \varphi_{dif} + \sum_{i=1}^{Ndof} \varphi_{rad,i} \tag{1}$$

Where Ndof is the number of degrees of freedom in the system (i.e. 6 times the number of floats). Due to the assumption of linearity a transformation can be made from time domain to frequency domain by applying a Fourier transform:

$$\hat{\varphi}(\omega) = \varphi(t)e^{-i\omega t} \tag{2}$$

Where ω is the frequency of the incident waves. A Boundary Element Method (BEM) is used where each velocity potential (except the incident wave potential, which is known) is described as a surface integral of source strengths and a Green function G:

$$\hat{\varphi}(\vec{x}, \omega) = \iint_S \sigma(\vec{\xi}, \omega) G(\vec{x}, \vec{\xi}, \omega) dS_\xi \tag{3}$$

The zero-speed Green function is used (Newman, 1985), which satisfies the linearised condition on the free surface and the no-flux condition on the seabed. The surface S on which sources are distributed is then reduced to the surfaces of the floats. These surfaces are discretized into N surface mesh elements and the source strengths are assumed constant on each mesh element. This results in the discretized version of equation (3):

$$\hat{\varphi}(\vec{x}, \omega) = \sum_{i=1}^{N} \sigma_i \iint_{S_i} G(\vec{x}, \vec{\xi}, \omega) dS_\xi \tag{4}$$

The magnitude of the source strengths on the mesh elements follows from applying the boundary condition for the radiation and diffraction potentials (no flux: water cannot go through the surface mesh) in the middle of each of the surface mesh elements. From the source strengths, pressures and velocities on surface mesh elements can be calculated. These are used to calculate wave forces and added mass and damping coefficients (A,B) which are then fed into the equation of motion of the floats to calculate the motion response:

$$\left(-(M + A)\omega^2 - iB\omega + C_{hydro} + C_{moor}\right)\vec{x} = \vec{F} \tag{5}$$

$\vec{x}$ is a vector with the 6DOF motion response of all floats. M, A, B, C_{hydro} are matrices with the dry inertia of the system, added mass, damping and hydrostatic restoring. $\vec{F}$ is a collection of external forces wave forces. C_{moor} is the stiffness matrix due to the surface mooring and hinges between the FPV modules. Once the motion response vector $\vec{x}$ is obtained, wave drift forces are calculated based on direct pressure integration (Pinkster 1979). Also hinge and surface mooring loads can be obtained by calculating relative motions between floats and multiplying with the appropriate stiffness.